Protein Structures

DOI: 10.1002/ange.200500540

Structural Interplay between Calcium(II) and Copper(II) Binding to S100A13 Protein**

Fabio Arnesano, Lucia Banci, Ivano Bertini, Adele Fantoni, Leonardo Tenori, and Maria Silvia Viezzoli*

S100s are dimeric proteins that constitute one of the largest groups in the EF-hand Ca^{II}-binding protein family.[1] The relevance of S100 proteins is shown by their involvement in various human diseases, through a variety of networks of interacting proteins.[1]

Human S100A13 is a ubiquitous protein of 98 amino acids which represents one of the latest members identified in the S100 protein family.[2] S100A13 is involved in the cellular export of interleukin-1α (IL-1α), a potent proinflammatory cytokine, and of fibroblast growth factor-1 (FGF-1), which plays a crucial role in angiogenesis and tissue regeneration.[3] Export is based on the Cu^{II}-dependent formation of multiprotein complexes containing the S100A13 protein, which assemble near the inner surface of the plasma membrane.

The primary sequence indicates that, like most S100 proteins, S100A13 contains a 12-residue canonical Ca^{II}-binding loop (site II) and a 14-residue "pseudo" Ca^{II}-binding loop (site I). The affinity of the two Ca^{II}-binding sites is 1.25×10^5 and $2.5 \times 10^3\,M^{-1}$, respectively.[4] Consistent with its function and its intracellular location near the inner surface of the plasma membrane, the Ca^{II}-binding affinity of site I of S100A13 is lower ($\approx 10^3\,M^{-1}$) than that typically found for other S100 proteins ($\approx 10^5$–$10^6\,M^{-1}$), as it is tuned for the higher local Ca^{II} ion concentration near the membrane.[5]

Herein, we report the structural effects of Ca^{II} and Cu^{II} ion binding to S100A13, and show that binding of two Ca^{II} ions per monomer triggers key conformational changes leading to the creation of two identical and symmetrical Cu^{II}-binding sites on the surface of the protein, close to the interface between the two monomers. These Cu^{II}-binding sites are unique among the S100 proteins, which are reported to bind Cu^{II} or Zn^{II} ions in addition to Ca^{II} ions.[6,7]

The expressed S100A13 was treated with ethylenediaminetetraacetic acid (EDTA) to remove all bound metal ions. Its molecular weight, as measured from electrospray

[*] Dr. F. Arnesano, Prof. L. Banci, Prof. I. Bertini, A. Fantoni, L. Tenori, Prof. M. S. Viezzoli
Magnetic Resonance Center CERM and Department of Chemistry
University of Florence
Via L. Sacconi 6, 50019 Sesto Fiorentino (Italy)
Fax: (+39) 055-457-4271
E-mail: bertini@cerm.unifi.it

[**] This work was supported by the European Commission (SPINE contract QLG2-CT-2002-00988). The Italian MURST COFIN03 is acknowledged for financial support.

Supporting information for this article is available on the WWW under http://www.angewandte.org or from the author.

mass spectra (ES-MS), is 11340 ± 1 Da, which corresponds to residues 2–98 (with the N-terminal methionine residue cleaved). Gel-filtration chromatography gives an apparent molecular mass of 25500 ± 500 Da, which indicates that the protein is in a dimeric state. Addition of Ca^{II} to the apoprotein (apo), followed by electronic spectroscopy,[4] produced a final species whose molecular weight was greater by 80 Da, thus confirming that the protein contains two bound Ca^{II} ions per monomer (Ca_2-S100A13).

The ^1H,^{15}N heteronuclear single-quantum coherence (HSQC) NMR spectra showed well-dispersed signals in both dimensions, indicative of a well-folded protein for both apo and Ca-loaded states, with a larger spectral dispersion for the latter (see Supporting Information). The ^{15}N relaxation measurements are consistent with a dimeric state of both forms of the protein in solution. They are characterized by overall rotational correlation times of 13.4 ± 1.2 and 15.0 ± 0.9 ns for the apo and Ca-loaded forms, respectively, and by the same rotational diffusion tensor ($D_{\parallel}/D_{\perp} = 1.2$).

Sequence-specific assignment was not complete for the backbone resonances of some of the residues at the C terminus ($R^{88}KKKDLKIRKK^{98}$) because of the high number of Lys and Arg residues determining extensive signals overlap. These residues experience negative $^{15}N\{^1H\}$ NOE values, which indicates a mobility faster than protein tumbling. The ^1H–^{15}N cross-peaks of residues 22–27 (corresponding to the first Ca^{II}-binding loop between helices α1 and α2) are sensitive to pH and disappear at pH values higher than 6.5 in both forms of the protein. The signals for residues 22–27 appear at lower pH values, but in the apo form they are split in multiple lines, thus indicating multiple conformations in slow exchange on the NMR timescale. This is not the case for Ca_2-S100A13, where residues 22–27 are stabilized toward a single conformation by calcium. Therefore, a complete dynamic characterization can be performed for the latter system. In total (residues 2–87), about 89 and 94% of carbon atoms, 90 and 95% of nitrogen atoms, and 86 and 91% of protons were assigned for apo- and Ca_2-S100A13, respectively (see Supporting Information).

The structures have backbone root-mean-square deviation (RMSD) values to the mean monomeric structure (residues 8–86) of 0.94 ± 0.41 and 0.58 ± 0.09 Å for apo- and Ca_2-S100A13, respectively. These values are 1.05 and 0.69 Å, respectively, for the dimer, for which the relative orientation of the two subunits has been experimentally determined through several intermonomer NOEs. The mean structures are shown in Figure 1a and b. A statistical analysis of the quality is reported in the Supporting Information. Both forms consist of homodimers, in which the two monomers are related by a twofold symmetry axis. Each monomer encompasses four α helices and two short β strands, in agreement with the chemical shift index. The two proposed Ca^{II}-binding sites are located between helices α1 and α2, and between helices α3 and α4, respectively (inset of Figure 1b), while a hinge region (residues 45–55) separates α2 from α3. A short antiparallel β sheet is identified within each monomer between residues S^{32} and S^{34} in Ca^{II}-binding site I, and residues E^{70} and K^{72} in site II. The ^1H,^{15}N amide chemical-shift differences between apo- and Ca_2-S100A13 are larger

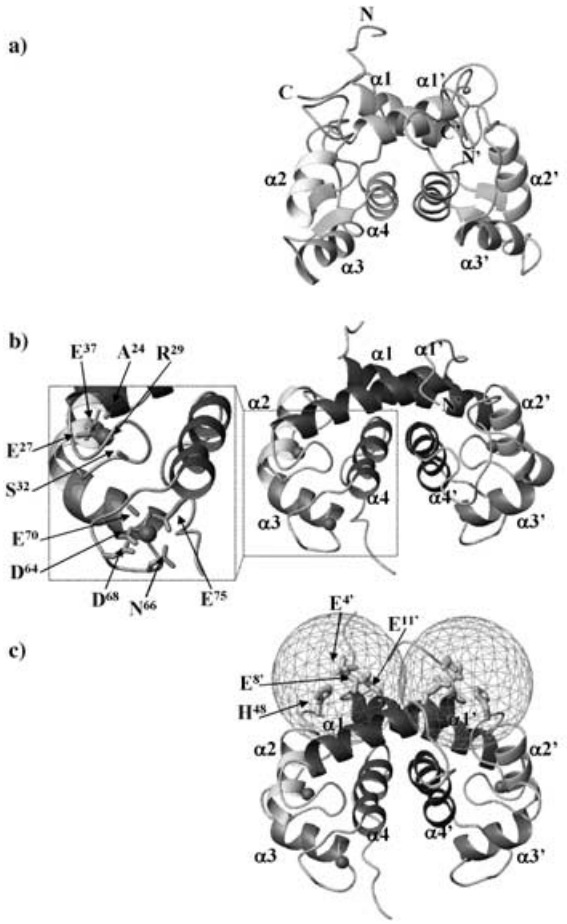

Figure 1. Dimeric structures of a) apo-S100A13 and b) Ca_2-S100A13 in solution are represented as ribbons, where each helix within a monomer has a different gray scale. Secondary structure elements are indicated. The two Ca^{II}-binding sites and Ca^{II} ligands are shown in the inset of (b). Ca^{II} ions are represented as spheres. c) Two 10-Å spheres are drawn on the structure of Ca_2-S100A13, which contain all residues whose signals are broadened beyond detection in the ^1H–^{15}N HSQC spectrum of Ca_2,Cu-S100A13. The potential Cu^{II} ligands of one site are indicated.

than average ($\Delta\delta_{av}(HN) > 0.37$ ppm) for segments 23–35, 60–70, and 77–82 (see Supporting Information), that is, where the two proposed Ca^{II}-binding sites are located. The extreme N terminus and the last ten residues of the C terminus are poorly defined as a result of their fast internal mobility, revealed by the small or negative $^{15}N\{^1H\}$ NOE values, which determines the lack of long-range interproton NOE values. Mutational studies have shown that deletion of the basic residues at the C terminus dramatically alters the ability of S100A13 to associate with the acidic protein partner FGF-1,[8] which suggests that the C terminus of S100A13 may become structured upon interaction with FGF-1.

Dimerization occurs through interactions between helices α1 and α4 of both monomers, which form an X-type bundle. At the dimer interface, residues in the hinge between α2 and α3 make contacts with residues near the N terminus of helix α1′ of the other monomer. The aromatic residues Y^{76} and W^{77} in helix α4 also make several contacts with helices α1′ and α4′ of the other monomer. All these interactions align α1

and α4 in opposite directions to α1′ and α4′, respectively, in the dimer. The angle between helices α4 and α4′ (160 ± 5°) in apo-S100A13 is larger than that in Ca_2-S100A13 (145 ± 5°), while helices α1 and α1′ form a similar angle (155 ± 5°). Also, the relative orientation of helices α1 and α2 is similar in the two forms (125 ± 5°). In contrast, the angle between helices α3 and α4 changes by ≈40°. In combination with α4–α4′ reorientation, this latter change has the dramatic effect of placing helix α3 nearly perpendicular to helix α4 (110 ± 5°) in the Ca^{II}-bound structure (Figure 1b), whereas they make an angle of 150 ± 5° in the apo form. The overall structure and the conformational changes induced by Ca^{II} binding are essentially the same as those observed for other S100 proteins.[1,9–11]

One result of the reorientation of helices is the exposure of several residues (see Supporting Information). In the S100 proteins characterized up to now this reorientation exposes a hydrophobic surface,[11] while in S100A13 the majority of the residues that become exposed are positively or negatively charged. They are located at the N termini (E^4, P^5, and E^{14}) and C termini (E^{86}, K^{89}, D^{92}, L^{93}, K^{94}, I^{95}, R^{96}, and K^{97}). Some residues in the hinge between helices α2 and α3 (P^{47}, H^{48}, K^{51}, and D^{52}) also become sizably exposed upon Ca^{II} binding. In particular, residue H^{48} increases its exposure by nearly 40%. However, some residues (mostly hydrophobic) become more buried upon Ca^{II} binding. As a consequence of the decreased exposure of residues 23–27 in Ca_2-S100A13, helix α1 becomes more extended at the C-terminal end, also resulting in a switch of residue packing. All these changes on the surface modify the electrostatic potential of the protein (Figure 2). The protein surface is highly charged in both forms, but the charge distribution appears quite different. In particular, at the dimer interface a more extended and continuous negative patch surrounded by positive charges is observable in Ca_2-S100A13 on top of helices α1 and α1′.

Interaction with Cu^{II} is a key functional aspect of S100A13, as this protein is reported to interact with other proteins in the presence of Cu^{II} ions. Indeed, it is involved in the Cu^{II}-mediated release of FGF1-1 and IL-1α.[3] On addition of a solution of $CuSO_4$ to Ca_2-S100A13 up to a ratio of 0.9:1, an absorption band appears at 720 nm and the ES-MS data indicate a mass increase of 63 Da, still maintaining the two Ca^{II} ions bound per monomer. The EPR spectrum of Ca_2,Cu-S100A13 is characterized by parameters $g_{\parallel} = 2.35$, $g_{\perp} = 2.07$, and $A_{\parallel} = 148 \times 10^{-4}\,cm^{-1}$. These data indicate a type II, pseudotetragonal coordination of Cu^{II} with N and O as donor atoms.[12]

The coupling between the unpaired electron of a type II Cu^{II}, characterized by electronic relaxation times in the range of 10^{-8}–10^{-9} s, and the nuclear spins has a dramatic effect on their nuclear relaxation and consequently on the NMR signal line widths.[13] Addition of substoichiometric amounts of copper to Ca_2-S100A13 results in the disappearance of a number of amide ^1H–^{15}N cross-peaks (residues 3, 4, 7–9, 11, 15, 48, and 49; see Supporting Information). From the location of the disappearing signals and line broadening analysis of the surrounding NH resonances,[13] the copper binding site can be located in a position equidistant from the hinge connecting helices α2 and α3 (residues 44–55) of one monomer and the N-terminal region of the other monomer (Figure 1c). The ^{15}N and ^{13}C NMR spectral data, confined in a well-defined region, also clearly indicate that the protein structure is not affected by the copper binding, as it is a secondary structural element, and the overall protein fold is maintained. It might also be possible that there is not a single binding site in the absence of the partner proteins, as some signal broadening occurs on residues located in the C terminus and close to the C-terminal calcium-binding site.

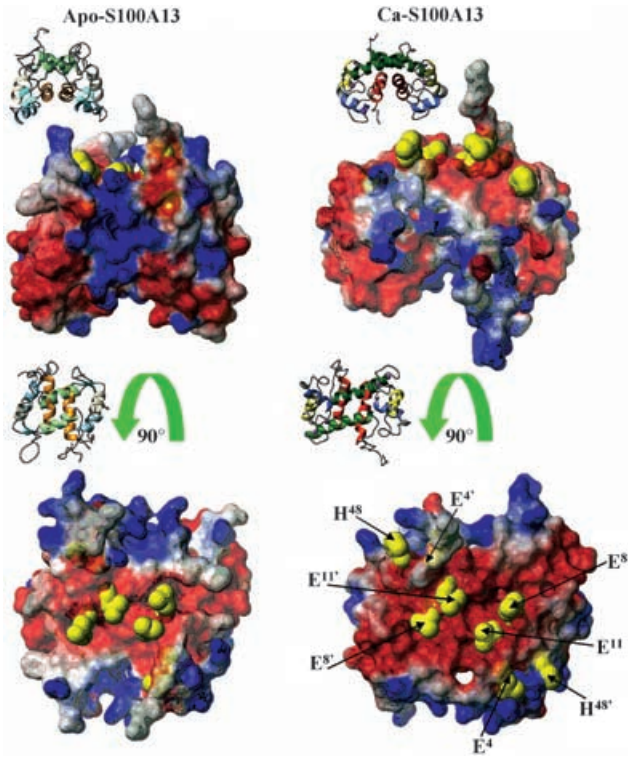

Figure 2. Rotated views of the electrostatic potential surface and ribbon representations of apo- and Ca_2-S100A13. The positively charged, negatively charged, and neutral amino acids are represented in blue, red, and gray, respectively. The putative Cu^{II} ligands are shown in yellow to allow their different degrees of solvent exposure in apo- and Ca_2-S100A13 to be observed.

In principle, direct ^{13}C NMR detection offers advantages for the study of paramagnetic proteins because the paramagnetic dipolar contributions to nuclear relaxation depend on the square of the gyromagnetic ratio of the observed nucleus. Thus, going from ^1H to ^{13}C detection guarantees a decrease in relaxation rates of a factor of about 16 ($\gamma_H = 2.67 \times 10^{-8}\,rad\,s^{-1}\,T^{-1}$; $\gamma_C = 6.73 \times 10^{-7}\,rad\,s^{-1}\,T^{-1}$), which therefore decreases the negative effects on the NMR signals arising from the paramagnetic nature of Cu^{II} ions.[14] Also, ^{13}C spectra are more sensitive than ^{15}N and ^1H spectra to even minimal changes of their environment, thus determining their power in monitoring structural perturbations. However, the presence of exchange processes can dramatically affect the ^{13}C signals determining their disappearance. In the CBCACO and CACO experiments[15] acquired on Ca_2-S100A13 in the presence of 0.9 equivalents of Cu^{II} ions (see Supporting Information) it appears that most of the carboxylate side chains of acidic residues disappear, presumably because of

their interaction with a fractional amount of copper in quasi-slow exchange. The disappearing signals on the backbone, however, are fully consistent with the ^{15}N spectral data, thus confirming that the Cu^{II} ion-binding site involves the N terminus region which is rich in glutamates (disappearance of ^{13}C backbone resonances of 3, 4, 6–9, 11) of one subunit and H^{48}, located in the loop between helices α2 and α3 (disappearance of its Cβ signal) of the other subunit.

The metal-binding site is completely different from that present in a few other S100 proteins where copper or zinc binding has been characterized.[6,7] The sites are different in their location on the protein frame, the nature of the ligand, and accessibility. That of S100A13 is completely exposed to solvent, which is in contrast to the situation in the other proteins where the site is quite buried.[6,7]

In conclusion, results of ^{15}N and ^{13}C NMR experiments have shown that Ca^{II} binding to S100A13 triggers sizable conformational changes, thus creating a novel binding site for Cu^{II} ions on a solvent-exposed location. The opening up of the interhelical angle α3–α4 and the uncovering of H^{48} in Ca_2-S100A13 (Figure 2) facilitate Cu^{II} binding at a site bridging the N terminus of one monomer with the hinge of the other monomer. This result suggests that Cu^{II} binding may trigger the interaction with biological partners and provide a mechanism for fine-tuning of the multiprotein complex that involves S100A13.

Experimental Section

The S100A13 recombinant protein was expressed in *Escherichia coli* by using cDNA from human brain, and purified by fast protein liquid chromatography. ^{15}N- and ^{13}C,^{15}N-labeled samples were obtained from cultures grown in labeled Silantes medium. All NMR experiments used for resonance assignment and structure determination were performed on 1.5 mM ^{13}C,^{15}N-S100A13 samples in sodium acetate buffer (20 mM, pH 5.6), and are summarized in the Supporting Information. Structure calculations were performed with DYANA,[16] calculated by using distance and dihedral angle constraints. Restrained energy minimization was then applied to the 25 conformers with the lowest DYANA target function, by using the AMBER 6 package.[17] The ^{15}N backbone longitudinal (R_1) and transverse (R_2) relaxation rates as well as heteronuclear $^{15}N\{^1H\}$ NOE values were measured as previously described.[18,19] 2D IPAP-CBCACO and CACO experiments based on direct ^{13}C NMR detection[15] were recorded for Ca_2-S100A13 and Ca_2,Cu-S100A13 on a 500-MHz spectrometer equipped with a TCI cryoprobe. Details on protein expression and characterization, NMR experiments, and structure calculations are available as Supporting Information.

Received: February 13, 2005
Revised: June 8, 2005
Published online: September 7, 2005

Keywords: calcium · copper · helical structures · NMR spectroscopy · protein structures

[1] I. Marenholz, C. W. Heizmann, G. Fritz, *Biochem. Biophys. Res. Commun.* **2004**, *322*, 1111–1122.
[2] R. Wicki, B. W. Schäfer, P. Erne, C. W. Heizmann, *Biochem. Biophys. Res. Commun.* **1996**, *227*, 594–599.
[3] I. Prudovsky, A. Mandinova, R. Soldi, C. Bagala, I. Graziani, M. Landriscina, F. Tarantini, M. Duarte, S. Bellum, H. Doherty, T. Maciag, *J. Cell Sci.* **2003**, *116*, 4871–4881.
[4] K. Ridinger, B. W. Schäfer, I. Durussel, J. A. Cox, C. W. Heizmann, *J. Biol. Chem.* **2000**, *275*, 8686–8694.
[5] S. McLaughlin, *Annu. Rev. Biophys. Biophys. Chem.* **1989**, *18*, 113–136.
[6] D. E. Brodersen, J. Nyborg, M. Kjeldgaard, *Biochemistry* **1999**, *38*, 1695–1704.
[7] O. V. Moroz, A. A. Antson, S. J. Grist, N. J. Maitland, G. G. Dodson, K. S. Wilson, E. Lukanidin, *Acta Crystallogr. Sect. D* **2003**, *59*, 859–867.
[8] M. Landriscina, R. Soldi, C. Bagala, I. Micucci, S. Bellum, F. Tarantini, I. Prudovsky, T. Maciag, *J. Biol. Chem.* **2001**, *276*, 22544–22552.
[9] L. Otterbein, J. Kordowska, C. Witte-Hoffmann, C. L. Wang, R. Dominguez, *Structure* **2002**, *10*, 557–567.
[10] L. Maler, M. Sastry, W. J. Chazin, *J. Mol. Biol.* **2002**, *317*, 279–290.
[11] S. Bhattacharya, W. J. Chazin, *Structure* **2003**, *11*, 738–739.
[12] J. Peisach, W. E. Blumberg, *Arch. Biochem. Biophys.* **1974**, *165*, 691–708.
[13] L. Banci, I. Bertini, C. Luchinat, *Nuclear and Electron Relaxation: The Magnetic Nucleus–Unpaired Electron Coupling in Solution*, VCH, Weinheim, **1991**.
[14] F. Arnesano, L. Banci, I. Bertini, I. C. Felli, C. Luchinat, A. R. Thompsett, *J. Am. Chem. Soc.* **2003**, *125*, 7200–7208.
[15] I. Bertini, L. Duma, I. C. Felli, M. Fey, C. Luchinat, R. Pierattelli, P. Vasos, *Angew. Chem.* **2004**, *116*, 2307–2309; *Angew. Chem. Int. Ed.* **2004**, *43*, 2257–2259.
[16] P. Güntert, C. Mumenthaler, K. Wüthrich, *J. Mol. Biol.* **1997**, *273*, 283–298.
[17] D. A. Case, D. A. Pearlman, J. W. Caldwell, T. E. Cheatham, W. S. Ross, C. L. Simmerling, T. A. Darden, K. M. Merz, R. V. Stanton, A. L. Cheng, J. J. Vincent, M. Crowley, V. Tsui, R. J. Radmer, Y. Duan, J. Pitera, I. Massova, G. L. Seibel, U. C. Singh, P. K. Weiner, P. A. Kollman, AMBER 6, University of California, San Francisco, **1999**.
[18] L. Banci, I. Bertini, F. Cantini, M. D'Onofrio, M. S. Viezzoli, *Protein Sci.* **2002**, *11*, 2479–2492.
[19] S. Grzesiek, A. Bax, *J. Am. Chem. Soc.* **1993**, *115*, 12593–12594.

